Meteorologische Zeitschrift, Vol. 22, No. 4, 463–470 (published online October 2013)

Open Access Article

Vertical velocity observed by Doppler lidar during cops – A case study with a convective rain event

JENNY DAVIS[1,*], CHRIS. COLLIER[1], FAY DAVIES[1], RALPH BURTON[1], GUY PEARSON[2] and PAOLO DI GIROLAMO[3]

[1]National Centre for Atmospheric Science, The University of Leeds, Leeds, UK
[2]Halo Photonics, Malvern, Worcester, UK
[3]Scuola di Ingegneria, Università degli Studi della Basilicata, Potenza, Italy

(Manuscript received July 11, 2012; in revised form June 20, 2013; accepted June 20, 2013)

Abstract

Convective and Orographically-Induced Precipitation Study (COPS), conducted in the Black Forest region in Southern Germany and Eastern France during the summer of 2007. From the 13 June to the 16 August 2007, the National Centre for Atmospheric Science (NCAS), Facility for Ground-based Atmospheric Measurement (FGAM) 1.5 μm scanning Doppler lidar was deployed at Super Site R, Achern, in the Rhine Valley, in order to contribute to the extensive COPS observation campaign. The FGAM Doppler lidar system provides measurements of radial wind and aerosol backscatter in the layer 100–1500 m. Profiles of horizontal wind velocity are presented, these being derived from performing azimuth scans. Profiles of vertical velocity, its variance and skewness derived from the vertical scans are also presented and discussed in the paper. Knowledge of vertical velocity skewness is important for the understanding of the structure and origin of turbulent convection in the atmospheric boundary layer (ABL). The skewness of vertical velocity can provide a measure of the asymmetry in the distribution of vertical velocity perturbations within the ABL and can be estimated using the Doppler lidar. In addition, we investigate the behaviour of the boundary layer using data from the FGAM Doppler lidar and Automatic Weather Station (AWS), the University of Basilicata Raman lidar (BASIL) and the DLR's Poldirad C-band radar. A case study event on the 6th August 2007 is selected and investigations of possible causes of layers with positive and negative skewness are presented, along with comparisons with output from the National Center for Atmospheric Research (NCAR) Weather Research and Forecasting (WRF) model to assess the accuracy of the model output, including location and timing of rainfall onset.

Keywords: Doppler lidar, convective rainfall, vertical velocity skewness.

1 Introduction

The COPS field campaign was conducted with the aim of advancing the quality of forecasts of convective and orographically-induced precipitation using extensive observations and modelling (COPS, 2007, WULFMEYER et al., 2008, 2011). One of the instruments deployed was the FGAM scanning 1.5 μm Doppler lidar system.

The Doppler lidar was collocated with an automatic weather station (AWS) at Supersite R (Achern, Lat: 48.64° N, Long: 8.06 E, Elev.: 140 m). The instruments were set up to run continuously from 13 June to 16 August 2007. The Doppler lidar is described in detail by BOZIER et al., 2007 and PEARSON et al., 2009. The aims and objectives of COPS are extensively described and discussed in WULFMEYER et al., 2008; KOTTMEIER et al., 2008; and WULFMEYER et al., 2011), and further analysis of lidar data from COPS is described in KALTHOFF et al. 2013.

*Corresponding author: Jenny Davis, National Centre for Atmospheric Science, The University of Leeds, Leeds LS2 9JT, UK, e-mail: j.davis@leeds.ac.uk

The first aim of the work was to produce a climatology for convective rainfall events, investigating wind speed, direction and the onset time of rainfall events, using the FGAM instruments. For the sake of brevity, details of this climatology are not discussed here. However, in summary, a convective rainfall event was defined as one where the prevailing winds were light, and there had been no rain that day before noon.

The second aim was to select, from the climatology study, one representative day when a convective rainfall event took place and to perform a more detailed analysis of the atmospheric processes leading up to that event. The selected case study was the Intensive Observation Period (IOP) 14a, on 6 August 2007, when convective cells were triggered in the Rhine Valley, followed later on by rain showers in the COPS area. For this specific case study an assessment of the vertical velocity variance and skewness has been carried out.

In previous studies HOGAN et al. (2009), LE MONE (1990), MOENG and ROTUNNO (1990) and MOYER and YOUNG (1991) noted that under fair-weather conditions,

DOI 10.1127/0941-2948/2013/0411
0941-2948/2013/0411 $ 3.60

when the ABL is heated from below, the skewness profile tends to be positive throughout the ABL, while under cloudy conditions the skewness profile can be affected by cloud processes and therefore be predominantly negative. Results from the selected case study are presented and discussed in the paper.

2 Measurements

The FGAM Doppler lidar is capable of providing measurements of the radial wind velocity and relative backscatter intensity. The system can also provide measurements of horizontal wind velocities from Velocity Azimuth Display (VAD) analysis (BROWNING and WEXLER, 1968), radial velocity variance and skewness, attenuated backscatter coefficient (β) at 1.5 μm and turbulent kinetic energy dissipation rate (ε). Section 4 of this work describes the method used for error analysis. Further, the accuracy of the instrument is discussed in detail by PEARSON et al. (2009) where it is concluded "values obtained show that in the atmospheric boundary layer, error of <10 cm^{-1} can be expected from the instrument. These values are sufficiently low that it is feasible to analyze the data further to extract detail such as the eddy dissipation rate, an important parameter difficult to measure by any other technique."

For signal processing, a certain amount of averaging is necessary as detailed by DAVIES et al. (2004). The FGAM Doppler lidar measures the return signal from a pencil-shaped volume of scatterers (primarily aerosol particles). The laser beam is collimated and has a transverse spatial dimension of ~0.1 m. For a fixed instant in time, the spatial extent of the lidar pulse along the transmit axis, Δr, given by the full-width half-maximum (FWHM) of the Gaussian profile of the pulse, is 18 m. For a radial velocity estimate from one of the laser's pulses, the illuminated aerosol region travels a distance, Δp, of 30 m. Therefore, the estimated velocity for a single pulse is a spatial average of the radial velocity, $v(r, t)$, over the sensing volume, where r is the range along the transmit axis and t is the time of measurement.

For multiple pulse measurements, as in this case study, the total measurement time (T), as detailed by FREHLICH and CORNMAN (2002) is:

$$T = \frac{N_P}{PRF} \tag{2.1}$$

where N_p is the number of accumulated pulses and PRF is the pulse repetition rate of the system. For this case study, the PRF was 20 kHz.

If the mean wind velocity is moving through the beam in a transverse direction, the lidar will sample a parallelogram of the atmosphere in a plane defined by the fixed laser beam and the fixed mean velocity vector. The transverse distance 'seen' by the Doppler lidar for each velocity estimate will be $\Delta h = V_H T$, where V_H is the mean transverse velocity.

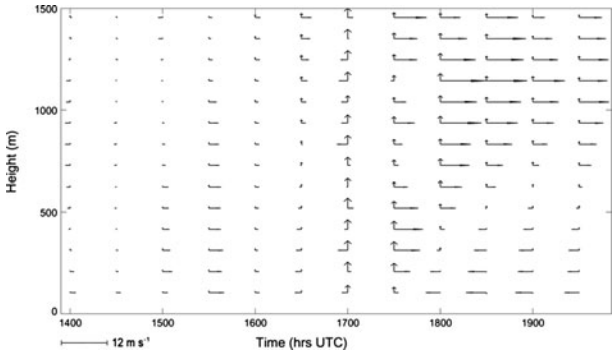

Figure 1: u and v velocity profiles derived from VAD analysis (BROWNING and WEXLER, 1968) of the Doppler lidar data on 06 August 2007. The arrows show the relative magnitude of the wind flow in the u and v directions. Modulus is ±9.95 m s^{-1}.

Each vertical velocity profile through the boundary layer (ray) was averaged over between 4–5 seconds, allowing the instrument time to process each ray. During much of the field campaign, the lidar system performed a series of pre-programmed scan patterns: vertical scans for 25 minutes at 90° and an azimuth scan with a duration of 5 minutes at 40° elevation.

The azimuth scans were performed to determine horizontal wind velocity profiles based on the application of the VAD analysis approach. On the 06 August 2007, the horizontal velocities measured reveal predominantly westerly winds, as suggested in Fig. 1. It can be seen that the u component of the winds below 1500 m throughout the early afternoon were relatively light, at around 2 m s^{-1}, with negligible contribution from the v component. The u wind velocity increases by 1530 hrs UTC, and at around 1630 hrs UTC turbulence appears to increase. At 1700 hrs UTC, the v component of the wind can be seen to have increased significantly, with the highest v velocities measured at around 1700 hrs UTC, prior to the rainfall event. After the event the wind velocity of both u and v components dropped to below 3 m s^{-1}.

Fig. 2 shows three profiles of potential temperature from the radiosonde ascents at (a) 1403 hrs UTC (solid line), showing a convective boundary layer, with z_i (mixed layer top) being approximately 1200 m, at (b) 1702 hrs UTC (dash-dot line) just prior to the rainfall event at Supersite R and (c) 2011 hrs UTC (dotted line) after the passing of the rainfall event, showing a stable boundary layer. Fig. 2(b) reveals the presence of an unstable layer up to approximately 700 m. Various inversions are present in the boundary layer at around 700 m, 1100 m, 1700 m and 2000 m. Comparing Fig. 2 with Fig. 3, it is considered that z_i here is approximately 1700 m, corresponding with the observed cloud base. Fig. 2(c) shows that by 2011 hrs UTC the boundary layer has lost its diurnal structure, however, residual layers can still be seen at around 1100 m and 1700 m.

Fig. 3 shows the temporal evolution of the boundary layer measured by the Doppler lidar on 06 August 2007.

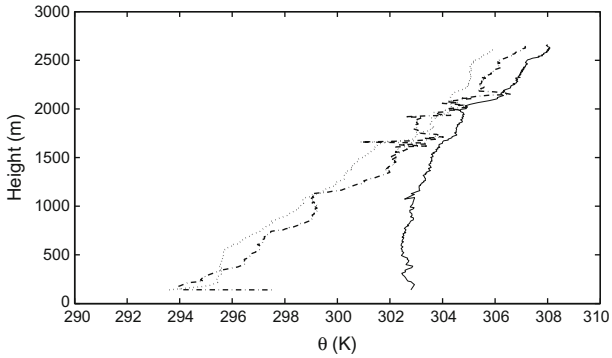

Figure 2: Vertical profiles of potential temperature derived from the radiosonde ascent on 06 August 2007, launched from Supersite R, Achern, at 1403 hrs UTC (solid line), 1702 hrs UTC (dash-dot line) and 2011 hrs UTC (dotted line). It is possible to see an unstable layer up to approximately 700 m at around 1702 hrs UTC, followed by a stable boundary layer at 2011 hrs UTC (c). It is suspected that the reason for cooling is a combination of the downdraft prior to the rainfall event, subsidence and cool advection of moist air.

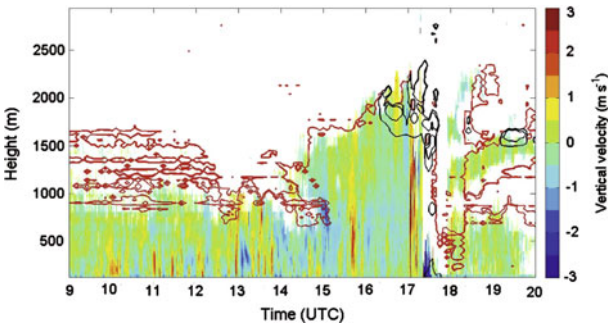

Figure 3: Vertical velocities 06 August 2007. Red contours show areas of low beta, black contours show clouds present. The strong negative vertical velocities at around 1730 UTC are resulting from rain.

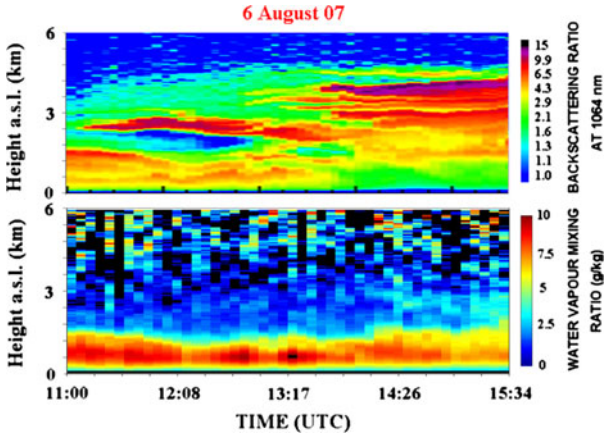

Figure 4: Temporal evolution of backscatter ratio and water vapour mixing ratio from the BASIL lidar at Supersite R for 06 August 2007, showing a clear air layer at around 2000 m. The upper panel represents the aerosol backscatter ratio at 1064 nm, while the lower panel represents the water vapour mixing ratio. Both panels show a descending layer from 1130 UTC.

Typically, on a clear-sky, convective day, the growth of thermals in the mixed layer is quite marked, with thermals reaching up to 1500 m or more. On this day, as shown in Fig. 3, despite the clear-sky conditions, thermals appear to be constrained to lower levels, with clear air, and therefore poor signal, above. This is shown by the lighter contours in Fig. 3. It is considered that the descending clear air layer loft is the reason why the thermals do not grow taller during this time. There are inversion layers present, which are shown in the radiosonde data (Fig. 2), likely resulting from the descending cold, clear layer. Fig. 3 also shows that between the times of 1200 UTC and 1430 UTC, a marked "clear air" layer with low backscatter signal has descended to around 900 m, as shown with red contours. Fig. 3 shows that by 1500 hrs UTC, this layer has cleared (shown in Figs. 3 and 4), allowing convective plumes to build during the late afternoon. The clear, dry layer was also recorded by other instruments based in the COPS study area that afternoon.

Specifically: Data from the University of Basilicata Raman lidar (BASIL, Di Girolamo et al., 2009), colocated at Supersite R is shown in Fig. 4. This shows a layer of clear, dry air between 1800 and 2400 m, descending from upper levels from 1345 UTC to 1500 UTC (lower panel of Fig. 4). Data here are expressed in terms of water vapour mixing ratio (g kg^{-1}). The upper panel of Fig. 4 shows the time evolution of the aerosol backscatter ratio at 1064 nm as measured by BASIL over the same time period;

The FGAM Wind Profiler, which was also located at this site, showed a clear air layer descending from around 1200 UTC until around 1430 UTC, with strong, upper level winds (above 1800 m) which descend to around 700 m from 1600 UTC onwards. The data from the Wind Profiler are not shown here, but they are in agreement with the VAD analysis and vertical velocities from the Doppler lidar. All the measurements suggest descending layers of clear air from upper levels.

The wind lidar (WiLi) from the Tropospheric Research Centre at Supersite M (to the east of Supersite R) recorded a layer of low SNR descending to between 1800 and 2100 m, later at 1400 UTC, which was also in agreement with BASIL. The data from WiLi are not shown here.

Fig. 3 also shows that at 1615 UTC clouds, shown with black contours, start to appear as, with the diurnal cycle, the land is heated and, as moister air approaches from the west, convective clouds are formed. At 1715 UTC, a large updraft is seen, which is followed by rainfall at 1730 UTC. The rain is seen in the Fig. as strong negative vertical velocity values as the target aerosols, considered to be tracers of wind velocity, are carried downwards. Here, the echoes from hydrometeors, both

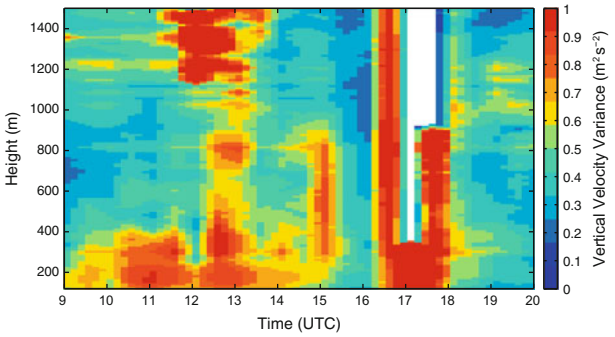

Figure 5: Temporal evolution of vertical velocity variance obtained from Doppler lidar measurements of vertical velocity, 06 August 2007, showing build up of thermals through the day, and rainfall, shown as high variance at 1730 UTC. The area of white at heights greater than 300 m at 1700 h UTC is where rainfall has removed scattering targets.

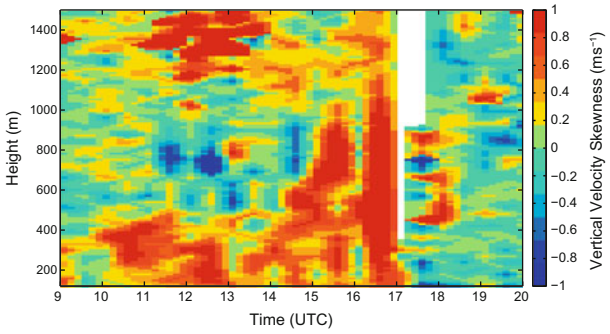

Figure 6: Temporal evolution of vertical velocity skewness obtained from Doppler lidar measurements of vertical velocity on 06 August 2007, showing layers of positive skewness being suppressed to below about 500 m before 1430 UTC, increasing in height prior to rainfall at 1730 UTC. As with Figure 5, the area of white at heights greater than 300 m at 1700 h UTC is where rainfall has removed scattering targets.

as cloud droplets and raindrops, are shown as darker contour lines progressively approaching surface at this time.

The following section outlines the data analysis performed for this case study. To investigate further the behaviour of the thermals prior to the rain event, vertical velocity variance and skewness were calculated.

3 Vertical velocity variance and skewness

The Doppler lidar is a useful instrument to study a volume of the atmosphere, the wind flow and its fluctuations contained within. The vertical velocity variance and skewness will now be discussed.

3a Variance

The vertical velocity variance from Doppler lidar data is shown in Fig. 5 and reveals the presence of thermally-driven turbulence, already depicted in Fig. 3. Variance of between 0.5 and 1 $m^2\ s^{-2}$ is shown confined to below 400 m through the morning. At around 1200 an inverted 'U-shaped' thermal structure, as described by WILLIAMS and HACKER (1992), HARROLD and BROWNING (1971) and BENNETT et al. (2006), can be seen in Fig. 3. This U-shape is visualised by the positive velocities (red) measured by the lidar, resulting from the surface being heated by the sun, and the consequent negative velocities (blue) as the air mass cools and descends. In the figure, the thermal at 12.00 UTC can be seen by the lidar to reach 1000 m in height as the aerosol 'targets' are only present up to this height.

Patches of high variance (between 0.5 and 1 $m^2\ s^{-2}$) can be seen at 800 m between 1230 and 1330 UTC and at 400 to 800 m at 1500 hrs UTC. The area of high variance at 1500 hrs UTC corresponds with the passing of the clear air layer shown in Fig. 3. A tall band of high variance is seen throughout the depth of the plot at 1630 UTC is thought to be associated with the start of the gust front approaching from the west. An area of high variance values between 1100 and 1500 m around 1200 UTC is the result of the noise associated with the clear layer present aloft and shown in Fig. 3 and Fig. 4.

The high variance values around 1500 UTC, reaching up to around 900 m are to be considered the result of a powerful thermal which can be seen to break through the inversions and the layers of clear air shown in Fig. 3. The high variance values found from 1615 UTC to 1800 UTC are to be interpreted as the result of turbulence triggered by the approaching gust front, which is followed by the rainfall event.

3b Skewness

Estimations of the vertical velocity skewness have been used to investigate the mechanisms driving turbulence processes observed on this day. Positive skewness values at the surface suggest narrow, intense updrafts at the surface, e.g. thermals, whereas negative skewness aloft suggests broad downdrafts associated with rainfall. Skewness has been estimated using the following equation (LE MONE, 1990; MOENG and ROTUNNO, 1990; MOYER and YOUNG, 1991; HOGAN et al., 2009):

$$s = \overline{w'^3} / \left(\overline{w'^2}\right)^{3/2} \qquad (3.1)$$

Fig. 6 illustrates the temporal evolution of the vertical velocity skewness as estimated from Doppler lidar data on the 06 August 2007. From 0900 UTC onwards, it is possible to reveal surface driven convection in the form of positive skewness. From around 1130 UTC to 1330 UTC, a band of negative skewness values is found between 500 m to 900 m, suggesting broad downdrafts. This band corresponds with the presence of the inversion layers from 700 m upwards as measured by the radiosonde launched at 1403 UTC (Fig. 2) and the presence

of a clear air layer descending from above. These inversion layers can inhibit convection and cause broad downdrafts, leading to the layer of negative skewness estimated at that time.

Two bands of strong positive skewness are observed from 1500 UTC to 1700 UTC. The first one at around 1530 UTC corresponds to the powerful thermals shown in Figs. 3, 5 and 6. The second one, at around 1615 UTC, is most likely caused by the gust front approaching from West and preceding the rainfall. Layers of positive and negative skewness values can be observed between 1100 UTC and 1400 UTC in the vertical region 1100–1600 m. These can be attributed to system noise associated with the previously discussed clear layer intrusions.

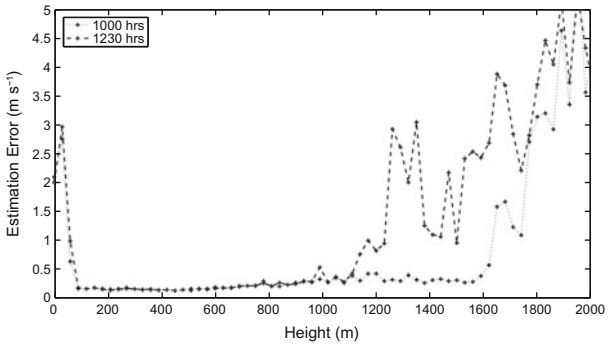

Figure 7: Estimation error of radial velocity for the FGAM Doppler lidar calculated from the velocity differencing procedure for 1000 – 1030 hrs UTC and 1230 – 1300 hrs UTC on the morning of 06 August 2007.

4 Error analysis

The analysis of errors affecting the FGAM Doppler lidar measurements has recently been documented by PEARSON et al. (2009). The error affecting the estimates of vertical velocity is a function of the lidar parameters, the atmospheric conditions and the velocity estimation procedure. It is therefore important to know the combined effect of the lidar parameters and the velocity estimation algorithm when performing measurements with this system (DAVIES et al., 2004).

FREHLICH (2001) noted that the effective wind velocity, $v_m(r)$, is a volume average over the pulse duration and range gate of the true line-of-sight (LOS) wind velocity, $v_t(r)$. The equation to be used to quantify wind velocity at range, r, and time, t, is the following:

$$v_r(r,t) = v_m(r,t) + e(r,t) + bias(r,t) \qquad (4.1)$$

where $e(r, t)$ is any error affecting the measurement and where the possibility of a range and time dependent bias, $bias(r, t)$, is also considered.

As discussed by PEARSON et al. (2009), the possibility of a bias for this instrument was investigated by analysing multiple 25-minute-long records of vertical velocity for 'no convection' periods since, in this case, the average vertical velocity should be close to zero. It was found that the average vertical velocity for these periods was consistently within ±0.06 m s^{-1}, indicating the presence of minimal bias in the velocity measurements (PEARSON, 2010).

FREHLICH (2001) described different techniques for deriving the error $e(r, t)$. In the present work the velocity differencing technique described by FREHLICH (2001) was used as it was previously found to have the best performance and lead to the smallest error (DAVIES et al., 2004). Two velocity estimates are taken, v_{even} and v_{odd}, from the data of even- and odd-numbered pulses, respectively. For a fixed beam geometry, the two sets of estimates will have the same desired measurement, $v(r, t)$ and the same minimal bias, provided no unusual events are present (for example, no rare cloud events and stationary statistics for the wind field and aerosol backscatter). Then, the difference of the two estimates $\Delta v(r, t, N/2) = v_{even}(r, t, N/2) - v_{odd}(r, t, N/2)$ can be written as:

$$\Delta v\left(r,t,\frac{N}{2}\right) = e_{even}\left(r,t,\frac{N}{2}\right) - e_{odd}\left(r,t,\frac{N}{2}\right) \qquad (4.2)$$

If we assume that e_{even} and e_{odd} are statistically similar and uncorrelated, the variance of gets the form:

$$\sigma^2_{\Delta v}\left(r,\frac{N}{2}\right) = 2\sigma^2_e\left(r,\frac{N}{2}\right) \qquad (4.3)$$

Therefore:

$$\sigma^2_e\left(r,\frac{N}{2}\right) = \frac{1}{2}\sigma^2_e\left(r,\frac{N}{2}\right) = \frac{\sigma^2_{\Delta v}}{4} \qquad (4.4)$$

Fig. 7 shows a plot of the estimated errors for two sets of data, one taken between 1000 h UTC and 1030 h UTC, the other between 1230 h UTC and 1300 h UTC and following the above mentioned methodology. The figure depicts that the error is relatively constant with range for ranges smaller than 1000 m and progressively increasing for larger ranges, as a result of the decreasing signal-to-noise ratio (SNR) with range. However, it is clearly visible that the range characterized by limited errors (smaller than 0.5 m s^{-1}) has decreased by approximately 500 m by 1230 h UTC. This coincides with the descent of the clear air layer from above.

5 Discussion and comparison of measurements with model output

The horizontal wind field measurements shown in Fig. 1 suggested westerlies until after the rainfall event, which was measured by the AWS between 1730 UTC and 1800 UTC. At that time the u wind velocity dropped to

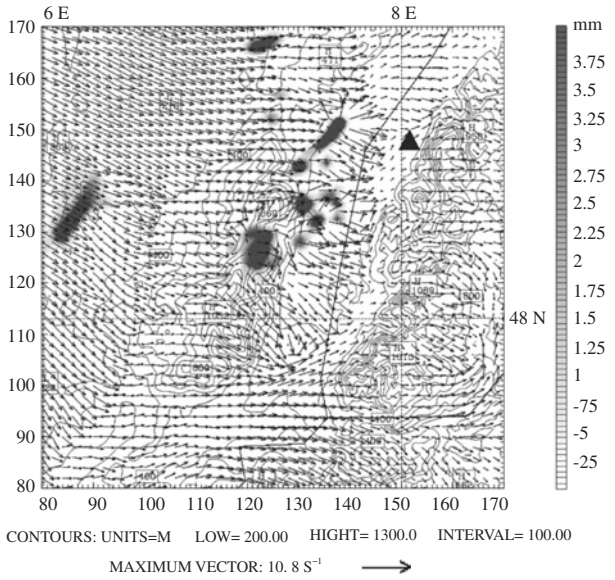

Figure 8: WRF output for 1700 UTC on 06 August 2007. The black triangle shows the location of Supersite R, the arrows represent the wind velocity vectors and the shaded areas represent rainfall. The solid contours represent height above mean sea level.

below 3 m s^{-2} and the direction backed to southerly at the surface. Higher up, the wind speed was larger (in excess of 10 m s^{-2}) and the direction was westerly to north-westerly. To investigate this further, the WRF model output was examined for this case study.

The Weather Research Forecasting (WRF) model is a state-of-the-art numerical weather prediction system, developed principally by NCAR and other US institutions and agencies (SKAMAROCK et al., 2009). In this case (Fig. 8), the output shows a gust front/outflow at 1700 UTC at z = 400 m. This appears to indicate an outflow from a convective rainfall event in the Vosges Mountains to the south and west of Supersite R. WRF results suggest that the higher wind velocities occur to the west of Supersite R, at that time, as shown in Fig. 8.

In order to ascertain whether rainfall events occurred to the west at that time, data from Poldirad was examined (not shown here). It was found that a storm system was moving north-east across the Vosges and into the Rhine Valley, further south and finally reaching Supersite R between 1730 UTC and 1800 UTC, which is consistent with the AWS data and confirming the likelihood of a gust front preceding the rainfall at Supersite R.

The vertical velocities measured throughout the day by the Doppler lidar showed thermals building in the mixed layer, but suppressed by the inversions between 700 m to 1100 m and the cool, dry layer above. However, a powerful thermal at around 1530 UTC appears to break through the inversion layers, and soon after that, clouds can be seen at 1615 UTC. The outflow gust appears to arrive at Supersite R at 1700 UTC, and at 1730 UTC strong negative velocities, shown in Fig. 3, suggest the occurrence of rainfall events, which are consistent with the AWS and Poldirad measurements. The model output indicates rainfall at Supersite R, but at a slightly later time (2000 UTC). This discrepancy in the timing on the precipitation between observations and WRF is perhaps unsurprising. In fact, it documented that the WRF (and other numerical weather prediction model) results are potentially sensitive to changes in microphysical schemes (GALLUS and PFEIFER, 2008), boundary-layer and surface schemes (BURTON et al., 2013, KHODAYAR and SCHÄDLER, 2013) and other physical parameterisations, which govern the distribution of moisture in the atmosphere.

The noise contribution to the retrieved radial velocity has been calculated following the velocity differencing technique (FREHLICH, 2001), which has been outlined earlier. The approximate size of the variance due to noise varies throughout the day, but for the periods shown in Fig. 7 was less than 0.5 m s^{-1}. However, the vertical range of low error estimates reduces from approximately 1600 m to approximately 1100 m with the descent of the clear air layer.

Further investigations of data from other lidars at COPS also suggest an intrusion of clear, dry air aloft. This is shown in the lower panel of Fig. 4 where data from BASIL shows a particularly pronounced clear, dry layer which is visible at ~800 m from 1130 UTC to 1430 UTC. This is evident both in the aerosol backscatter field (upper panel of Fig. 4) and in the water vapour mixing ratio field (lower panel of Fig. 4). These observations coincide with the features observed by the FGAM Doppler lidar showing suppression of the boundary layer top by a layer of dry air aloft.

The vertical velocity variance illustrated in Fig. 5 highlights the increasing turbulence strength at Supersite R, as expected because of the thermals growth in height and intensity. The high values of variance measured in the afternoon suggest an increase in the height of the turbulent layer starting around 1500 UTC, as the powerful thermals break through the low level inversions. Again, high variance values are observed just prior to the rainfall event at 1730 UTC. It is to be considered that this increase in turbulence intensity could be attributed to an outflow gust from the rainfall events to the west of Supersite R, as suggested by the WRF simulation (Fig. 8). The variance is plotted up to 1500 m as beyond that height the signal becomes too noisy.

The vertical velocity skewness, shown in Fig. 6, is restricted by noise to a maximum height of 1500 m, similarly to the vertical velocity variance shown in Fig. 5. Measurements suggest that surface driven turbulence processes are present up to a height of ~500 m, with negative skewness values becoming more evident around noon, as a possible result of the descending clear air layer and inversions shown in Figs. 2, 3, and 4. The layered structure of skewness at around 1200 UTC, at heights above 1200 m, is considered to be caused by low signal returns from the lidar due to the descending clear air layer. Importantly though, shortly after 1500 UTC, skewness becomes predominantly positive throughout the boundary layer to a raised elevation of around 1000 m.

This is attributed to the large thermals observed at 1530 UTC. The gust later on, at 1700 h UTC, is also expressed as strong positive skewness values. Without any knowledge on the horizontal and vertical velocities, it may be straightforward to interpret the strong positive skewness values at around 1700 UTC as a result of thermals. However, the high horizontal velocities measured at that time suggest a gust/outflow event, as also indicated by WRF and shown in Fig. 7. The rainfall event reaching Supersite R at 1730 UTC is interpreted as associated with the gust front.

6 Conclusions

The present paper provides a case study for convective rainfall event recorded at Supersite R (Achern, Southern Germany) by the FGAM instruments (Doppler lidar and AWS) during COPS in the time frame June-August 2007.

It was found that during the 62 days of measurements, there were 46 days where rain fell. Of these, convective rainfall, characterised by dry mornings and rainfall onset later in the afternoon, occurred on 11 days. Generally, wind direction was observed to be between westerly and south-westerly, with wind speed increasing before the rainfall event.

The event on the 6th August 2007 was characterized by the highest amount of rainfall recorded, and which is considered here to investigate for the possible causes of observed layers of positive and negative skewness values.

Convection on 06 August 2007 is thought to have been suppressed by several low level inversions, which are observed in the radiosonde potential temperature data.

A descending clear, dry layer aloft was observed by the FGAM Doppler lidar and by BASIL at Supersite R and at the same time Doppler and backscatter lidars at Supersite M made observations of very low aerosol backscatter

During the afternoon, an outflow/gust and deep convection occurred followed by rain. The rainfall event on 06 August 2007 was observed by the FGAM AWS and D.L.R.'s C-band Poldirad radar. The associated precursors and after-effects of the rainfall event on windflow were recorded by the FGAM Doppler lidar.

Measurements of skewness profiles through the boundary layer are not well documented in the literature but can be measured using Doppler lidar, as described herein. Skewness measurements provide good additional data for investigating the drivers of turbulence. However, these must be used with care, as they can still be ambiguous without additional information. Surface-driven positive vertical velocity skewness at low levels (<500 m) has been recorded, but between 1130 h UTC and 1330 h UTC, negative skewness is recorded at around 750 m, coinciding with the intrusion of clear air, and noise above. Positive skewness values observed around 1400 UTC can be associated with surface convection and are measured up to 1000 m and higher until the rainfall event at 1730 UTC.

The velocity-differencing error analysis method described by FREHLICH (2001) provided an effective tool to infer the maximum height for the vertical velocity measurements to be considered reliable. This was found to be 1500 m at 1000 h UTC, reducing to 1100 m at 1230 h UTC, this latter corresponding with the clear air intrusion.

Results are presented along with comparisons with output from the WRF model. This shows clouds, but rainfall is not found to occur until three hours after the gust front. To explore the full WRF sensitivity of this test case to the various combinations of physical schemes, and to the initialisation, would constitute an extensive study and is beyond the scope of the present work. However, it is supposed that the present results are representative, and further work to improve the onset time of precipitation would not produce results which differ greatly in terms of the underlying dynamical response.

Acknowledgments

The funding for the participation in COPS was provided as part of the NERC UK COPS consortium.

The FGAM scanning 1.5 μm Doppler lidar system was built by Halo Photonics and funded by the N.C.A.S. Facility for Ground-based Atmospheric Measurement (FGAM) through the UK Natural Environment Research Council.

The authors would like to thank Dr. E. NORTON at Manchester University for the provision of the wind profiler data, Dr. M. HAGEN at DLR for the provision of Poldirad data and Dr. D. ALTHAUSEN from the Leibniz Institute for Tropospheric Research for the provision of Wili data.

References

BENNETT, L.J., K.A. BROWNING, A.M. BLYTH, D.J. PARKER, P.A. CLARK, 2006: A review of the initiation of precipitating convection in the United Kingdom. – Quart. J. Roy. Meteor. Soc. **132**, 1001–1020.

BOZIER, K.E., G.N. PEARSON, C.G. COLLIER, 2007: Doppler lidar observations of Russian forest fire plumes over Helsinki. – Weather **62**, 203–208.

BROWNING, K.A., R. WEXLER, 1968: The Determination of Kinematic Properties of a Wind Field using Doppler Radar. – Quart. J. Roy. Meteor. Soc. **97**, 283–299.

BURTON, R.R., A. GADIAN, A. BLYTH, S.D. MOBBS, 2013: Modelling isolated deep convection: a case study from COPS. – Meteorol. Z. **22**, 433–443. DOI:10.1127/0941-2948/2013/0408.

DAVIES, F., C. COLLIER, G.N. PEARSON, K. BOZIER, 2004: Doppler Lidar Measurements of Turbulent Structure Function over an Urban Area. – J. Atmos. Oceanic Technol. **21**, 753–761.

DI GIROLAMO, P., D. SUMMA, R. FERRETTI, 2009: Rotational Raman Lidar measurements for the characterization of stratosphere-troposphere exchange mechanisms. – J. Atmos. Oceanic Technol. **26**, 1742–1762.

FREHLICH, R., 2001: Simulation of coherent Doppler lidar performance for space-based platforms. – J. Appl. Meteor. **39**, 245–262.

FREHLICH, R., L. CORNMAN, 2002: Estimating spatial velocity statistics with coherent Doppler lidar. – J. Atmos. Oceanic Technol. **19**, 355–366.

GALLUS, W.A., M. PFEIFER, 2008: Intercomparison of simulations using WRF microphysics schemes with dual-polarization data for a German squall line. – Advan. Geosci. **16**, 109–116.

HARROLD, T.W., K.A. BROWNING, 1971: Identification of preferred areas of shower development by means of high-power radar. – Quart. J. Roy. Meteor. Soc. **97**, 330–339.

HOGAN, R.J., A.L.M. GRANT, A.J. ILLINGWORTH, G. PEARSON, E. O'CONNOR, 2009: Vertical velocity variance and skewness in clear and cloud-topped boundary layers as revealed by Doppler lidar. – Quart. J. Roy. Meteor. Soc. **135**, 635–643.

KALTHOFF, N., K. TRÄUMNER, B. ADLER, S. SPÄTH, A. BEHRENDT, A. WIESER, J. HANDWERKER, F. MADONNA, V. WULFMEYER, 2013: Dry and moist convection in the boundary layer over the Black Forest - a combined analysis of in situ and remote sensing data. – Meteorol. Z. **22**, 445–461. DOI:10.1127/0941-2948/2013/0417.

KHODAYAR, S., G. SCHÄDLER, 2013: The impact of soil moisture variability on seasonal convective precipitation simulations. Part II: sensitivity to land-surface models and prescribed soil type distributions. – Meteorol. Z. **22**, 507–526. DOI:10.1127/0941-2948/2013/0431.

KOTTMEIER, C., N. KALTHOFF, C. BARTHLOTT, U. CORSMEIER, J. VAN BAELEN, A. BEHRENDT, R. BEHRENDT, A. BLYTH, R. COULTER, S. CREWELL, P. DI GIROLAMO, M. DORNINGER, C. FLAMANT, T. FOKEN, M. HAGEN, C. HAUCK, H. HOLLER, H. KONOW, M. KUNZ, H. MAHLKE, S. MOBBS, E. RICHARD, R. STEINACKER, T. WECKWERTH, A. WIESER, 2008: Mechanisms initiating deep convection over complex terrain during COPS. – Meteorol Z. **17**, 931–948. DOI:10.1127/0941-2948/2008/0348.

LE MONE, M.A., 1990: Some observations of Vertical Velocity Skewness in the Convective Planetary Boundary Layer. – J. Atmos. Sci. **47**, 1163–1169.

MOENG, C.H., R. ROTUNNO, 1990: Vertical-Velocity Skewness in the Buoyancy-Driven Boundary Layer. – J. Atmos. Sci. **47**, 1149–1162.

MOYER, K.A., G.S. YOUNG, 1991: Observations of Vertical Velocity Skewness within the Marine Stratocumulus-Topped Boundary Layer. – J. Atmos. Sci. **48**, 403–410.

PEARSON, G., 2010: Halo-Photonics. – Personal Communication.

PEARSON, G., F. DAVIES, C. COLLIER, 2009: An analysis of the performance of the UFAM pulsed Doppler lidar for observing the boundary layer. – J. Atmos. Oceanic Technol. **2**, 240–250.

SKAMAROCK, W.C., J.B. KLEMP, J. DUDHIA, D.O. GILL, D.M. BARKER, M.G. DUDA, X.Y. HUANG, W. WANG, J.G. POWERS, 2009: A description of the Advanced Research WRF Version 3 – NCAR Tech. Note TN-475+STR.

WILLIAMS, A.G., J.M. HACKER, 1992: Interactions between coherent eddies in the lower convective boundary layer. – Bound.-Layer Meteor. **64**, 55–74.

WULFMEYER, V., A. BEHRENDT, 2007: COPSfield report v2.1, with contribution of G. ADRIAN, D. ALTHAUSEN, F. AOSHIMA, J. VAN BAELEN, C. BARTHLOTT, H.-S. BAUER, A. BLYTH, C. BRANDAU, U. CORSMEIER, G. CRAIG, S. CREWELL, G. DICK, M. DORNINGER, Y. DUFOURNET, G. EHRET, R. ENGELMANN, C. FLAMANT, T. FOKEN, C. HAUCK, P. DI GIROLAMO, H. GRAßL, M. GRZESCHIK, J. HANDWERKER, M. HAGEN, R.M. HARDESTY, C. HAUCK, W. JUNKERMANN, N. KALTHOFF, C. KIEMLE, C. KOTTMEIER, L. KRAUSS, C. LONG, J. LELIEVELD, F. MADONNA, M. MILLER, S. MOBBS, B. NEININGER, S. PAL, G. PETERS, M. RADLACH, E. RICHARD, M. ROTACH, H. RUSSCHENBERG, P. SCHLÜSSEL, U. SCHUMANN, C. SIMMER, R. STEINACKER, D. TURNER, S. VOGT, H. VOLKERT, T. WECKWERTH, H. WERNLI, A. WIESER, C. WUNRAUM. – COPS, https://www.uni-hohenheim.de/spp-iop/documents/COPSFieldReport2.pdf.

WULFMEYER, V., A. BEHRENDT, H.-S. BAUER, C. KOTTMEIER, U. CORSMEIER, A. BLYTH, G. CRAIG, U. SCHUMANN, M. HAGEN, S. CREWELL, P. DIGIROLAMO, C. FLAMANT, M. MILLER, A. MONTANI, S. MOBBS, E. RICHARD, M.W. ROTACH, M. ARPAGAUS, H. RUSSCHENBERG, P. SCHLUSSEL, M. KONIG, V. GARTNER, R. STEINAKER, M. DORNIGER, D.D. TURNER, T. WECKWERTH, A. HENSE, C. SIMMER, 2008: Research campaign The Convective and Orographically-induced Precipitation Study: A Research and Development Project of the World Weather Research Programme for improving quantitative precipitation forecasting in low-mountain regions. – Bull. Amer. Meteor. Soc. **89**, 1477–1486. DOI:10.1175/2008BAMS2367.1.

WULFMEYER, V., A. BEHRENDT, C. KOTTMEIER, U. CORSMEIER, C. BARTHLOTT, G.C. CRAIG, M. HAGEN, D. ALTHAUSEN, F. AOSHIMA, M. ARPAGAUS, H.-S. BAUER, L. BENNETT, A. BLYTH, C. BRANDAU, C. CHAMPOLLION, S. CREWELL, G. DICK, P. DI GIROLAMO, M. DORNINGER, Y. DUFOURNET, R. EIGENMANN, R. ENGELMANN, C. FLAMANT, T. FOKEN, T. GORGAS, M. GRZESCHIK, J. HANDWERKER, C. HAUCK, H. HÖLLER, W. JUNKERMANN, N. KALTHOFF, C. KIEMLE, S. KLINK, M. KÖNIG, L. KRAUSS, C.N. LONG, F. MADONNA, S. MOBBS, B. NEININGER, S. PAL, G. PETERS, G. PIGEON, E. RICHARD, M.W. ROTACH, H. RUSSCHENBERG, T. SCHWITALLA, V. SMITH, R. STEINACKER, J. TRENTMANN, D.D. TURNER, J. VAN BAELEN, S. VOGT, H. VOLKERT, T. WECKWERTH, H. WERNLI, A. WIESER, M. WIRTH, 2011: The Convective and Orographically-induced Precipitation Study (COPS) the scientific strategy, the field phase, and research highlights. – Quart. J. Roy. Meteor. Soc. **137**, 3–30. DOI:10.1002/qj.752.